Bulletin of the Seismological Society of America. Vol. 59, No. 2, pp. 591–601. April, 1969

THE RELATION BETWEEN FAULT PLANE SOLUTIONS FOR EARTHQUAKES AND THE DIRECTIONS OF THE PRINCIPAL STRESSES

By Dan P. McKenzie

ABSTRACT

The stresses involved in shallow earthquakes and their occurrence along fault planes suggest that they occur by failure on weak planes, rather than by brittle fracture of a homogeneous material. Possible orientations of the stress tensor are examined to determine what limits fault plane solutions can place on the orientation of the greatest principal stress. For the general case of a triaxial stress, the only restriction is that this stress direction must lie in the quadrant containing *P*, but may be at right angles to the *P* direction. Thus shallow earthquakes impose a few limitations on the orientation of the stress tensor. In contrast the fault plane solutions from deep earthquakes are best explained by fracture of a homogeneous material, with the greatest principal stress directed down the dip of the earthquake zone.

Introduction

The state of stress within the Earth has always been of interest to geology and geophysics. The folding and thrusting observed in orogenic belts demonstrates that a nonhydrostatic stress field must have been present during the formation of mountain belts, though it is difficult to estimate from the geology the magnitude of the stress required. Since it is now clear that most earthquakes are produced by slip on faults, the occurrence of earthquakes to depths of about 700 km is also evidence of a nonhydrostatic stress field. The seismic waves radiated from an earthquake may be used to estimate both the magnitude and the orientation of the principal stresses in the hypocentral region. The purpose of this paper is to discuss the limitations of such estimates, and in particular those obtained from fault plane solutions.

A good account of the theory of faulting is given by Anderson (1951). He starts from the assumption that the rock is initially homogeneous and fault free. If a triaxial stress field is applied to such a material at room temperature and pressure it fails by slip on either of two planes containing the intermediate stress axis, and inclined at an angle of 45° or less to the greatest principal stress. Various experiments (Griggs and Handin, 1960) have demonstrated that geological materials do fail in this way, though often at angles considerably less than 45°. Anderson suggested that the orientation of the stress axes could be obtained from that of the failure or fault plane. This simple argument cannot apply to most earthquakes for two reasons. The first is that when earthquakes produce surface displacements they almost always do so along preexisting faults. For instance the earthquake whose fault plane solution is shown in Figure 1 took place on the North Anatolian fault in Eastern Turkey. A similar phenomenon is the control of the deformation of superficial rocks by faults in the underlying basement. The other difficulty is that the shear stresses involved in shallow earthquakes are at least an order of magnitude too small to produce fracture (Chinnery, 1964; Brune and Allen, 1967, Wyss and Brune, 1968). These observations strongly suggest that a fault, once established, is a plane of weakness, and that later movements are not simply related to the principal stress directions. These objections do not apply to the application of Anderson's ideas to the first faults formed in a homogeneous body of material, for instance a granite batholith involved for the first time in orogenic movements.

These remarks suggest that it is more realistic to enquire what orientation and magnitude of principal stresses would produce slip in the observed direction on the earthquake fault plane, rather than to require this plane also to be a plane of failure. These more general conditions must of course contain the failure conditions as a special case.

The mechanism of earthquakes has been studied extensively using fault plane solutions (see Stauder, 1962, for instance). Such solutions are now best obtained from the direction of the *P*-wave onset on the vertical world wide long period seismographs established by the U. S. Coast and Geodetic Survey. The *P*-wave data is often combined with the direction and polarization of the *S*-wave onset. The direction in which the rays left the focus may then be obtained from the angular distance between the source and receiver and the hypocentral depth. Since the path of each ray depends on the velocity structure of the Earth, the calculated angle between the ray and the horizontal is affected by any uncertainties in the velocity structure, or alternatively in the focal depth. This problem principally affects solutions for shallow earthquakes, because velocity gradients are large in the crust. It is convenient to imagine a sphere centered on and surrounding the focus on which the first-motion directions are plotted, and then to project the lower hemisphere into a horizontal plane using either a stereographic or an equal area projection. Fault-plane solutions may also be obtained from surface waves (Brune, 1961) and from the amplitude of free oscillations (Gilbert and MacDonald, 1961), but are generally less reliable than those obtained from first motions.

A large number of such fault plane solutions now exist. Wickens and Hodgson (1967) give a collection of those from before 1962, and many more (Stauder and Bollinger, 1966a, b; Sykes, 1967, for instance) have since been made using the long period WW SSN stations. Unfortunately few of the short-period solutions made before 1962 are reliable for reasons discussed by Stevens and Hodgson (1968). However all reliable solutions at all depths obtained so far are consistent with a double couple source. Thus all earthquakes studied so far could be caused by slip on a fault. Figure 1 shows an example of such a solution for an earthquake in Eastern Turkey and demonstrates how the compressions and dilatations are separated into quadrants by two orthogonal planes. One of these planes is the fault plane, the other is the auxiliary plane. There is no method of deciding which is the fault plane from either the *P* or the *S* observations. This ambiguity is fundamental to the double-couple source mechanism. There are, however, several methods of determining which is the fault plane. If the earthquake produces a surface break on a fault, then the displacement and fault plane observed must correspond with one of the planes in the mechanism solution. The earthquake in Figure 1 accompanied such a surface break on the North Anatolian fault, and the motion was principally right-handed strike slip (Wallace, 1968). The strike of the principal surface break is shown and agrees well with both the strike and the sense of motion of one of the planes, which is therefore the fault plane. Most earthquakes do not accompany a surface break on land, and therefore the choice must be made by different methods. McKenzie and Parker (1967) used the horizontal projection of the slip vector for this purpose, which they showed was consistent over large regions if the slip was in the fault plane rather than the auxiliary plane. The distribution of aftershocks, the radiation pattern as a function of frequency and the ellipticity of the isoseismal lines may also be used to remove the ambiguity.

Various authors (Hodgson, 1957; McIntyre and Christie, 1957; Scheidegger, 1964; Shirokova, 1967) have believed in the importance of some direction which is uniquely determined by the fault-plane solution, such as the *P* or the *T* axis, or the null-motion direction. Since the ambiguity depends on the use of distant stations and is not a feature of the fault motion, there is no physical argument to support this belief. Indeed, the success of the ideas of paving stone tectonics (McKenzie and Parker, 1967; Morgan, 1968) demonstrates that it is essential to choose between the fault plane and the auxiliary plane. Throughout the analysis below it will be assumed such a choice has been made, though it is easy to generalize the results if such a choice is impossible.

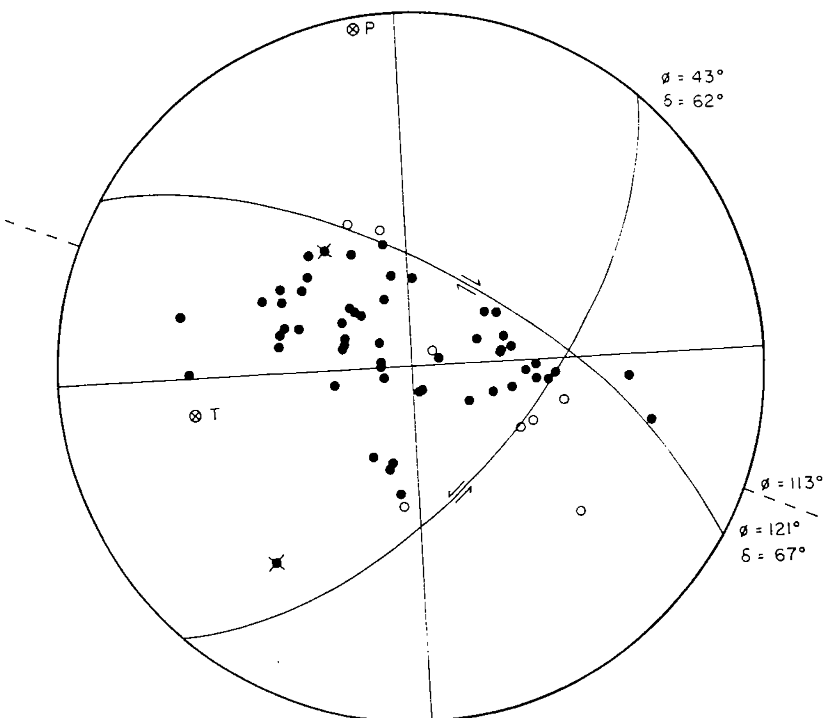

FIG. 1. Fault plane solution for the shock of August 19, 1966 in Eastern Turkey. Diagram is an equal area projection of the lower hemisphere of the radiation field. Solid circles represent compressions, open circles dilations, crosses indicate station is near a nodal plane. ϕ and δ are the strike and dip of the nodal planes, and arrows indicate the sense of motion. The dotted line shows the strike of the major right lateral surface break which accompanied the earthquake.

THEORY

The slip vector **u** of one side of the fault relative to the other must lie in the fault plane with normal **n**. Thus **n**, **u** and **n** × **u** are three orthogonal vectors, and it is convenient to discuss the orientation of the stress tensor which produces the slip with respect to these axes rather than to a set related to the vertical. Defining **n**, **u** and **n** × **u** as the x_1, x_2 and x_3 axes respectively (Figure 2), the fault plane is $x_1 = 0$ and the half space $x_1 < 0$ moves in the $+x_2$ direction relative to $x_1 > 0$. The P axis of the fault-plane solution is then the direction (1, 1, 0) and the T axis in the direction (1, −1, 0). The null vector (Hodgson, 1957) is the x_3 axis and $x_2 = 0$ is the auxiliary plane. The analysis below determines which orientations of the stress tensor will produce slip in the positive x_2 direction. The only assumption introduced is that the slip vector **u** is always parallel to the resolved shearing stress in the fault plane. This assumption is physically reasonable if the rock was originally homogeneous. If the stress tensor is $\mathbf{S}'$ or (S'_{ij}) in the focal plane coordinate system, then the force on the fault plane is given by

$$\mathbf{F} = \mathbf{S}' \cdot \mathbf{n}. \tag{1}$$

The shearing component of **F**, **f** is given by

$$\mathbf{f} = \mathbf{n} \times [(\mathbf{S}' \cdot \mathbf{n}) \times \mathbf{n}]. \tag{2}$$

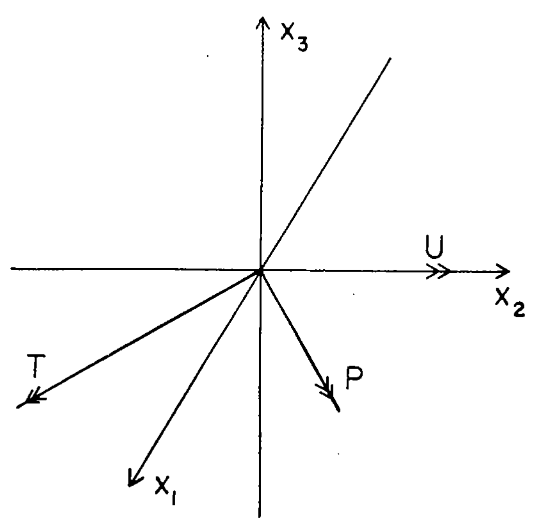

FIG. 2. The coordinate axes determined by the fault plane solution. $x_1 = 0$ is the fault plane, and slip of $x_1 < 0$ occurs in the positive x_2 direction with respect to $x_1 > 0$.

Since **u** is parallel to **f**

$$\mathbf{u} \times \mathbf{f} = \mathbf{u} \times [\mathbf{n} \times ([\mathbf{S}' \cdot \mathbf{n}] \times \mathbf{n})] = 0. \tag{3}$$

With the particular choice of axes discussed above (3) reduces to

$$S'_{13} = 0. \tag{4}$$

The shearing stress on the fault plane which produces the slip is S'_{12}. The purpose of the matrix analysis which follows is to determine what orientations of the principal axes of the stress tensor will satisfy both (4) and the condition on the direction slip.

If the reference frame is not specified the stress tensor may always be written

$$\mathbf{S} = \begin{bmatrix} -S_1 & 0 & 0 \\ 0 & -S_2 & 0 \\ 0 & 0 & -S_3 \end{bmatrix} \tag{5}$$

where

$$S_1 \geqq S_2 \geqq S_3 .$$

(5) is equivalent to

$$\mathbf{S} = -\begin{bmatrix} \sigma_1 & 0 & 0 \\ 0 & \sigma_2 & 0 \\ 0 & 0 & 0 \end{bmatrix} - S_3 \mathbf{I} \tag{6}$$

where

$$\sigma_1 = S_1 - S_3 , \qquad \sigma_2 = S_2 - S_3 , \qquad \sigma_1 \geqq \sigma_2$$

and $\mathbf{I}$ is the unit matrix. In this problem, however, the reference frame is not arbitrary, but is defined by the fault-plane solution. In this coordinate system the stress tensor $\mathbf{S}'$ is

$$\mathbf{S}' = \mathbf{A}^{-1}\mathbf{S}\mathbf{A}. \tag{7}$$

$\mathbf{A}$ is a unitary matrix which transforms the arbitrary reference frame into that defined by the fault plane; it is equivalent to a rotation about some axis. Thus

$$\mathbf{A}^{-1} = \mathbf{A}^{T}. \tag{8}$$

It is more useful to write (7) using the Einstein summation convention over repeated indices

$$S'_{ij} = S_{kl}A_{lj}A_{ki} . \tag{9}$$

Alternatively, (9) may be written

$$S'_{ij} = S_{kl}B_{jl}B_{ik} \tag{10}$$

where

$$\mathbf{B} = \mathbf{A}^{-1} \tag{11}$$

and transforms the fault-plane reference frame into that defined by the principal axes of the stress tensor. $\mathbf{B}$ may be expressed in terms of successive rotations $\mathbf{B}_1$, $\mathbf{B}_2$ and $\mathbf{B}_3$ through angles θ, $-\phi$ and ψ about the x_1 , x_2 and x_3 axes, respectively

$$\mathbf{B} = \mathbf{B}_3\, \mathbf{B}_2\, \mathbf{B}_1 . \tag{12}$$

This choice carries the greatest principal stress into the positive octant.

The advantage of writing $\mathbf{B}$ in this way is that ϕ and ψ specify the orientation of the greatest principal stress, S_1 , of the stress tensor. (12) then gives

$$\mathbf{B} = \begin{bmatrix} \cos\psi\cos\phi, & -\cos\psi\sin\phi\sin\theta - \sin\psi\cos\theta, & -\cos\psi\sin\phi\cos\theta + \sin\psi\sin\theta \\ \sin\psi\cos\phi, & -\sin\psi\sin\phi\sin\theta + \cos\psi\cos\theta, & -\sin\psi\sin\phi\cos\theta - \cos\psi\sin\theta \\ \sin\phi, & \cos\phi\sin\theta, & \cos\phi\cos\theta \end{bmatrix}. \quad (13)$$

The condition expressed by (4) now becomes:

$$S'_{13} = -\sigma_1 B_{11} B_{13} - \sigma_2 B_{12} B_{23}$$

$$= -[\sigma_1 \cos\psi \sin\phi - \sigma_2 \sin\theta\,(\cos\psi\sin\phi\sin\theta + \sin\psi\cos\theta)]\cos\phi = 0. \quad (14)$$

(14) is satisfied if

$$\phi = (\pi/2) \quad (15)$$

$$\sigma_1 = 0, \qquad \theta = 0 \quad (16)$$

$$\sigma_2 = 0, \qquad \phi = 0 \quad (17)$$

$$\sigma_2 = 0, \qquad \psi = (\pi/2) \quad (18)$$

$$\frac{\sigma_1}{\sigma_2} = \sin^2\theta + \frac{\tan\psi}{\sin\phi}\sin\theta\cos\theta. \quad (19)$$

Only (19) permits a solution for general orientations of a triaxial stress tensor. (19) may also be written

$$\frac{2\sigma_1}{\sigma_2} - 1 = \alpha = \left(1 + \frac{\tan^2\psi}{\sin^2\phi}\right)^{1/2} \sin(2\theta - \chi) \quad (20)$$

where

$$\tan\chi = \frac{\sin\phi}{\tan\psi}. \quad (21)$$

Since the orientation of S_1, the greatest principal stress, does not depend on θ, (20) gives the accessible values of ψ and ϕ for S_1

$$\frac{\tan\psi}{\sin\phi} \geqq \sqrt{\alpha^2 - 1}. \quad (22)$$

Figure 3 shows, for various values of α, the directions in which S_1 may lie. Provided (22) is satisfied, (20) gives the two possible values of θ for given values of ψ and ϕ

$$\theta_1 = \frac{1}{2}\tan^{-1}\left(\frac{\sin\phi}{\tan\psi}\right) + \frac{1}{2}\sin^{-1}\left[\alpha \Big/ \left(1 + \frac{\tan^2\psi}{\sin^2\phi}\right)^{1/2}\right] \quad (23)$$

$$\theta_2 = \frac{\pi}{2} + \frac{1}{2}\tan^{-1}\Big(\ldots$$

If (22) is an equality $\theta_1 = \theta_2$, and
The expression for S'_{12} may also

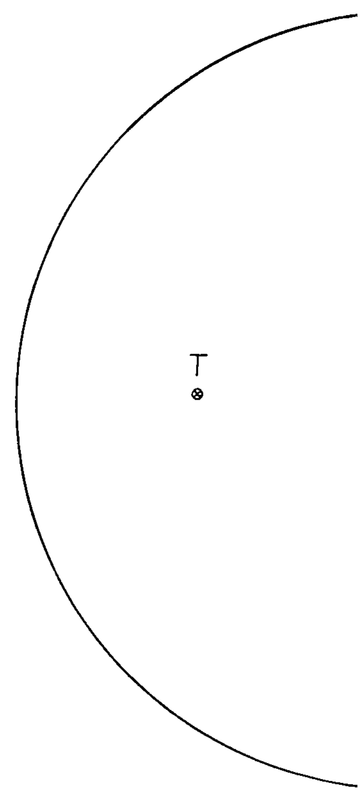

FIG. 3. An equal area projection of Fig
greatest principal stress S_1 for various va
the right of the curves are accessible to S

$$S'_{12} = -\sigma_1 B_{11} B_{21} - \sigma_2 B_{12} B_{22}$$

$$= -\sigma_1 \sin\psi\cos\psi\cos^2\phi$$

$$-\sigma_2(\cos\psi\sin\phi\sin\theta + \sin \ldots$$

If (19) is satisfied, (25) reduces to

$$S'_{12} = -\sigma_1 \ldots$$

where θ must have the value of θ_1 or

$$\theta_2 = \frac{\pi}{2} + \frac{1}{2}\tan^{-1}\left(\frac{\sin\phi}{\tan\psi}\right) - \frac{1}{2}\sin^{-1}\left[\alpha \bigg/ \left(1 + \frac{\tan^2\psi}{\sin^2\phi}\right)^{1/2}\right]. \tag{24}$$

If (22) is an equality $\theta_1 = \theta_2$, and both are imaginary if (22) is not satisfied.

The expression for S'_{12} may also be obtained from (10) and (13)

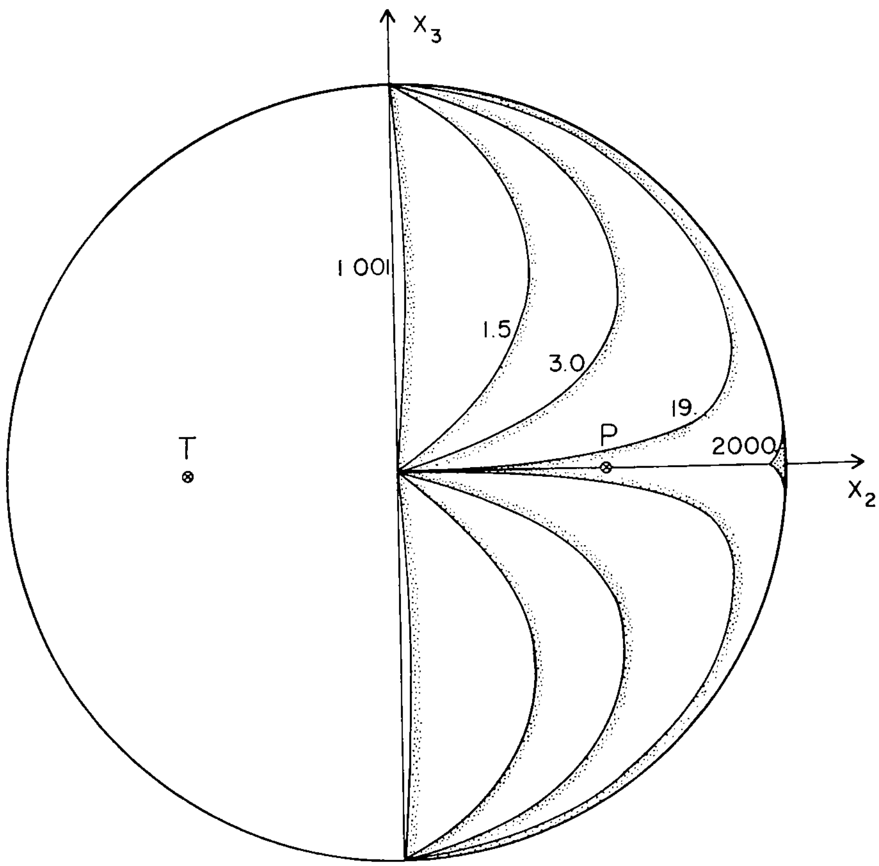

FIG. 3. An equal area projection of Figure 2 with axis x_1 to show the possible orientations of the greatest principal stress S_1 for various values of α or $(2S_1 - S_3 - S_2)/(S_2 - S_3)$. All regions to the right of the curves are accessible to S_1.

$$\begin{aligned} S'_{12} &= -\sigma_1 B_{11} B_{21} - \sigma_2 B_{12} B_{22} \\ &= -\sigma_1 \sin\psi \cos\psi \cos^2\phi \\ &\quad -\sigma_2 (\cos\psi \sin\phi \sin\theta + \sin\psi \cos\theta)(\sin\psi \sin\phi \sin\theta - \cos\psi \cos\theta). \end{aligned} \tag{25}$$

If (19) is satisfied, (25) reduces to

$$S'_{12} = -\sigma_1 \cos^2\psi \left(\tan\psi - \frac{\sin\phi}{\tan\theta}\right) \tag{26}$$

where θ must have the value of θ_1 or θ_2. In the special case when (22) is an equality:

$$\tan \theta = \sqrt{\frac{\alpha + 1}{\alpha - 1}} \tag{27}$$

and

$$S'_{12} = -\frac{\sigma_1}{2}\left(\frac{\alpha - 2}{\alpha - 1}\right) \sin 2\psi. \tag{28}$$

The other special case is $\phi = 0$, when S'_{12} can either be obtained from (14) and (25) directly, or by considering the limiting cases of (23), (24) and (26) as $\phi \rightarrow 0$. θ_1 gives

$$S'_{12} = -\left(\frac{\sigma_1 - \sigma_2}{2}\right) \sin 2\psi \tag{29}$$

and θ_2 :

$$S'_{12} = -\frac{\sigma_1}{2} \sin 2\psi. \tag{30}$$

Since $\sin \phi$ and $\tan \theta$ are always positive, and $\sigma_1 \geqq \sigma_1 - \sigma_2$, the greatest value of $| S'_{12} |$ is $\sigma_1/2$ and occurs when $\theta = (\pi/2)$, $\phi = 0$, $\psi = (\pi/4)$ or when S_1 coincides with the P axis, and S_2 with the null vector of the fault-plane solution. Figure 4 shows contours of $|(2S'_{12})/(\sigma_1)|$ when $(\sigma_1/\sigma_2) = 2$ and $\theta = \theta_2$. A similar diagram may be constructed for θ_1, but this has smaller shear stresses everywhere.

The remaining case (15) is $\phi = (\pi/2)$ and the greatest principal stress is parallel to the null vector. Then (25) gives

$$S'_{12} = \frac{\sigma_2}{2} \sin 2(\psi + \theta). \tag{31}$$

(16), (17) and (18) can only apply if two of the principal stresses are equal, and may be discussed in the same way. (17) corresponds to a uniaxial stress with $S_2 = S_3$. The shearing force is then determined by (25):

$$S'_{12} = -\frac{\sigma_1}{2} \sin 2\psi \quad \text{if} \quad \phi = 0. \tag{32}$$

Thus S_1 must lie in the $x_3 = 0$ plane. A similar result applies to S_3, the least principal stress, if $S_1 = S_2$.

Throughout this discussion it has been assumed that a choice between the fault and the auxiliary plane has been made. If such a choice is impossible the range of possible orientations of S_1 is even greater, and may be obtained from Figure 3 by reflecting the envelope for $(\pi/4) < \psi < (\pi/2)$ in the $\psi = (\pi/4)$ plane.

The special case when the fault plane is produced by failure of a homogeneous rock requires S_2 to lie along x_3 and S_1 to be in the $x_3 = 0$ plane, between the P and the x_1 axes. The angle γ between S_1 and P is determined by the coefficient of friction, μ, and is

$$\gamma = \tfrac{1}{2} \tan^{-1} \mu. \tag{33}$$

The results of this section show that S_1 must be in the dilatational quadrant of the

fault-plane solution, or within 90°
further restriction can be placed
uniaxial, or the fault lies in a prev
The mean-shear stress $\bar{\sigma}$ involv
1968; Wyss and Brune, 1968) is

$\bar{\sigma} =$

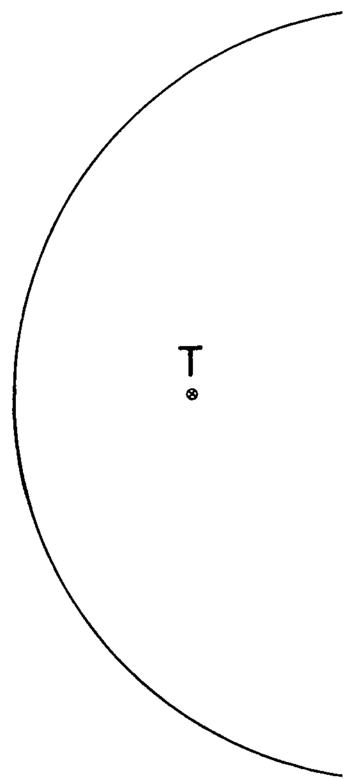

FIG. 4. An equal area projection of c
$\alpha = 3$ or $(S_1 - S_3)/(S_2 - S_3) = 2$. Cor
and are normalised to make the maxim

where τ is the time taken for the
S'_{12} show that $\bar{\sigma}$ generally provides
static stress involved in the earthq

The general theory shows that
capable of imposing only rather w
principal stress. This conclusion dis
they only considered faults formed
ternal friction. Their arguments are

fault-plane solution, or within 90° of the P axis. This result is not very useful, but no further restriction can be placed on the orientation of S_1 unless the stress tensor is uniaxial, or the fault lies in a previously unfaulted material.

The mean-shear stress $\bar{\sigma}$ involved in earthquakes (Brune and Allan, 1967; Brune, 1968; Wyss and Brune, 1968) is

$$\bar{\sigma} = \int_0^\tau S'_{12}(t)\, dt \Big/ \int_0^\tau dt$$

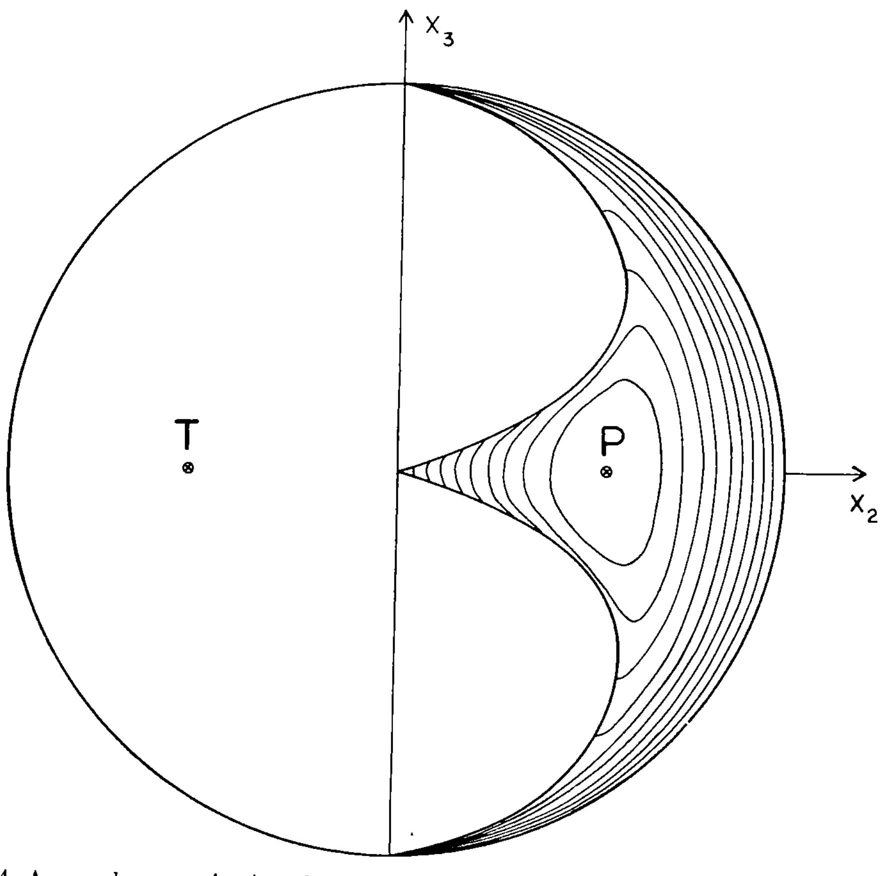

FIG. 4. An equal area projection of contours of the shearing stress S'_{12} in the $x_1 = 0$ plane when $\alpha = 3$ or $(S_1 - S_3)/(S_2 - S_3) = 2$. Contours are at intervals of .1 refer to the orientation of S_1 and are normalised to make the maximum of S'_{12}, on the P axis, unity.

where τ is the time taken for the elastic waves to be emitted. The expressions for S'_{12} show that $\bar{\sigma}$ generally provides an order of magnitude estimate of the nonhydrostatic stress involved in the earthquake.

APPLICATIONS

The general theory shows that fault plane solutions for shallow earthquakes are capable of imposing only rather weak restraints on the orientation of the greatest principal stress. This conclusion disagrees with the ideas of previous authors because they only considered faults formed by fracture of a homogeneous material without internal friction. Their arguments are then correct, but for the reasons discussed in the introduction such a model appears to be a poor one for shallow earthquakes. Previous attempts to relate either the null (Hodgson, 1957) or the P axes (Scheidegger, 1964, Shirokova, 1967) to the major features of the Earth's surface were not entirely unsuccessful because the slip vector is invarient and therefore the P axis only varies by 45° from this direction.

A more important application is to deep earthquakes. Isacks (Isacks *et al*, 1968, and personal communication) has demonstrated that the P axes of intermediate and deep focus earthquakes in the Tonga-Fiji and Kermadec regions are approximately parallel to the dip of the plane containing the earthquakes. Such clustering is more obvious for the P axes than for any other axes, though there is a weak orientation of T at right angles to the dipping plane. This result would not be expected if the earthquakes were caused by slip on pre-existing fault planes. It is best explained by failure of a homogeneous material with little internal friction. The observed fault-plane solutions then require the greatest principal stress to lie in the plane containing the earthquakes, and to be directed down the dip. The weak orientation of T is also explained if the intermediate stress lies along the strike of the plane. If this explanation is correct, values of $\bar{\sigma}$ comparable with the fracture strength of rocks, ~5kb, might be expected from deep earthquakes.

Acknowledgments

I am grateful to B. L. Isacks for stimulating my interest in the stress fields obtained from fault-plane solutions, and particularly those from deep focus earthquakes. M. Wyss suggested that the shear stresses involved could be large. This research was begun at Lamont Geological Observatory under NSF GP-1208 and was completed under a NASA fellowship.

Refferences

Anderson, E. M. (1951). *The Dynamics of Faulting*. Edinburgh, Oliver and Boyd.

Brune, J. N. (1961). Radiation pattern of Rayleigh waves from the Southeast Alaska earthquake of July 10, 1958, *Publ. Dom. Obs. Ottawa* **24**, 373–383.

Brune, J. N. (1968). Seismic moment, seismicity, and rate of slip along major fault zones, *J. Geophys. Res.* **73**, 777–784.

Brune, J. N. and C. R. Allen (1967). A low-stress-drop low-magnitude earthquake with surface faulting: The Imperial, California earthquake of March 4, 1966, *Bull. Seism. Soc. Am.* **57**, 501–514.

Chinnery, M. A. (1964). The strength of the Earth's crust under horizontal shear stress, *J. Geophys. Res.* **69**, 2085–2089.

Gilbert, F. and G. J. F. MacDonald (1961). Free oscillations of the Earth 1. Toroidal oscillations *J. Geophys. Res.* **65**, 675–693.

Griggs, D. and J. Handin (1960). Rock deformation, *Geol. Soc. Am. Memoir*, **79**.

Hodgson, J. H. (1957). The nature of faulting in large earthquakes, *Bull. Geol. Soc. Am.* **68**, 611–644.

Hodgson, J. H. (1959). The Null vector as a guide to regional tectonic patterns, *Publ. Dom. Obs. Ottawa* **20**, 369–384.

Isacks, B. L., J. Oliver and L. R. Sykes (1968). Seismic evidence for the motions of the Lithosphere, 1. Downward motion in island arcs, *Trans. Am. Geophys. Union* **49**, 282 (abs.).

McIntyre, D. B. and J. M. Christie (1957). A discussion of "The nature of Faulting in Large Earthquakes", *Bull. Geol. Soc. Am.* **68**, 645–652.

McKenzie, D. P. and R. L. Parker (1967). The North Pacific: an example of tectonics on a sphere, *Nature*, **216**, 1276–1280.

Morgan, W. J. (1968). Rises, trenches, great faults, and crustal blocks, *J. Geophys. Res.* **73**, 1959–1982.

Scheidegger, A. E. (1964). The tectonic stress and tectonic motion direction in Europe and Western Asia as calculated from earthquake fault plane solutions, *Bull. Seism. Soc. Am.* **54**, 1519–1528.

Shirokova, E. I. (1967). General fe in the Mediterranean-Asian *Earth*) 12–22 (eng. transl.).

Stauder, W. (1962). The focal mec

Stauder, W. and G. A. Bollinger (28, 1964, and its aftershock s

Stauder, W. and G. A. Bollinger (quakes of 1963, *Bull. Seism. S*

Stevens, A. E. and J. H. Hodgson Hodgson catalogue, *Bull. Sei*

Sykes, L. R. (1967). Mechanism o *J. Geophys. Res.* **72**, 2131–21

Wallace, R. E. (1968). Earthquak *Soc. Am.* **58**, 11–45.

Wickens, A. J. and J. H. Hodgson *Dom. Obs., Ottawa*, **33**, 1–56

Wyss, M. and J. N. Brune (1968). in the California-Nevada regi

Department of Geological an
Princeton University
Princeton, New Jersey 08540

Manuscript received July 29, 1

Shirokova, E. I. (1967). General features in the orientation of principal stresses in earthquake foci in the Mediterranean-Asian seismic belt, *Izv. Akad. Nauk S.S.S.R.* (*Physics of the Solid Earth*) 12–22 (eng. transl.).

Stauder, W. (1962). The focal mechanism of earthquakes, *Adv. in Geophys.* **9**, 1–76.

Stauder, W. and G. A. Bollinger (1966a). The focal mechanism of the Alaska earthquake of March 28, 1964, and its aftershock sequence, *J. Geophys. Res.* **71**, 5283–5296.

Stauder, W. and G. A. Bollinger (1966b). The *S*-wave project for focal mechanism studies, earthquakes of 1963, *Bull. Seism. Soc. Am.* **56**, 1363–1371.

Stevens, A. E. and J. H. Hodgson (1968). A study of *P* nodal solutions (1922–1962) in the Wickens-Hodgson catalogue, *Bull. Seism. Soc. Am.* **58**, 1071–1082.

Sykes, L. R. (1967). Mechanism of earthquakes and nature of faulting on the mid-oceanic ridges, *J. Geophys. Res.* **72**, 2131–2153.

Wallace, R. E. (1968). Earthquake of August 19, 1966. Varto area, Eastern Turkey, *Bull. Seism. Soc. Am.* **58**, 11–45.

Wickens, A. J. and J. H. Hodgson (1967). Computer re-evaluation of mechanism solutions, *Publ. Dom. Obs., Ottawa*, **33**, 1–560.

Wyss, M. and J. N. Brune (1968). Seismic moment, stress and source dimensions for earthquakes in the California-Nevada region, *J. Geophys. Res.* **73**, 4681–4694.

Department of Geological and Geophysical Sciences
Princeton University
Princeton, New Jersey 08540

Manuscript received July 29, 1968.